A Potent, Selective Inhibitor of Matrix Metalloproteinase-3 for the Topical Treatment of Chronic Dermal Ulcers

M. Jonathan Fray,*,† Roger P. Dickinson,† John P. Huggins,‡ and Nicholas L. Occleston‡,§

Departments of Discovery Chemistry and Discovery Biology, Pfizer Global Research and Development, Sandwich, Kent, CT13 9NJ, U.K.

Received February 6, 2003

The pathology of chronic dermal ulcers is characterized by excessive proteolytic activity which degrades extracellular matrix (required for cell migration) and growth factors and their receptors. The overexpression of MMP-3 (stromelysin-1) and MMP-13 (collagenase-3) is associated with nonhealing wounds, whereas active MMPs-1, -2, -9, and -14 are required for normal wound healing to occur. We describe the synthesis and enzyme inhibition profile of (3*R*)-3-({[(1*S*)-2,2-dimethyl-1-({[(1*S*)-2-methoxy-1-phenylethyl]amino}carbonyl)propyl]amino}-carbonyl)-6-(3-methyl-4-phenylphenyl)hexanoic acid (UK-370,106, **7**), which is a potent inhibitor of MMP-3 (IC_{50} = 23 nM) with >1200-fold weaker potency vs MMP-1, -2, -9, and -14. MMP-13, which may also contribute to the pathology of chronic wounds, was inhibited about 100-fold less potently by compound **7**. Compound **7** potently inhibited cleavage of [^{3}H]-fibronectin by MMP-3 (IC_{50} = 320 nM) but not cleavage of [^{3}H]-gelatin by either MMP-2 or -9 (up to 100 μM). Compound **7** had little effect, at MMP-3 selective concentrations, on keratinocyte migration over a collagen matrix in vitro, which is a model of the re-epithelialization process. Following iv (rat) or topical administration to dermal wounds (rabbit), compound **7** was cleared rapidly ($t_{1/2}$ = 23 min) from plasma, but slowly ($t_{1/2} \sim$ 3 days) from dermal tissue. In a model of chronic dermal ulcers, topical administration of compound **7** for 6 days substantially inhibited MMP-3 ex vivo. These data suggest compound **7** is sufficiently potent to inhibit MMP-3-mediated matrix degradation while leaving unaffected cellular migration mediated by MMPs 1, 2, and 9. These properties make compound **7** a suitable candidate for progression to clinical trials in human chronic dermal wounds, such as venous ulcers.

Introduction

The normal healing of wounds is a complicated process that proceeds through a number of well-defined and orchestrated stages.[1] First, blood loss is stemmed through blood coagulation and formation of a clot consisting of a fibrin mesh interwoven with activated platelets. Next, chemotactic and growth factors are released to attract neutrophils and macrophages that clear debris and bacteria from the wound and in turn amplify the initial wound healing signals by stimulating neighboring fibroblasts and keratinocytes to form granulation tissue. Fibroblasts proliferate and then invade the clot, laying down a provisional matrix of fibronectin and collagens to act as scaffolding for the subsequent reconstruction of the tissue, and endothelial cells form new capilliaries. Re-epithelialization is achieved by keratinocytes that migrate and proliferate at the interface between healthy dermis and the granulation tissue, thereby covering the wound site. Once a new keratinocyte monolayer is established, epidermal migration ceases and a new stratified epidermis with associated basal lamina develops. Re-epithelialization is made easier by contraction of the underlying connective tissue, which brings the wound margins toward each other.

The process of acute wound healing is usually complete in about two weeks, although further tissue remodeling continues over many months. In contrast, chronic dermal wounds such as venous ulcers, diabetic ulcers, and pressure sores can take many months to heal.[2] Some persist indefinitely, and in certain circumstances amputation of part of the affected limb is required. Chronic dermal wounds are a cause of much suffering and impose a significant financial burden on healthcare providers.[3]

The standard treatment for venous ulcers consists of cleaning the wound and applying pressure bandaging once weekly.[4] Newer approaches comprise administration of growth factors (e.g., Regranex, recombinant human platelet-derived growth factor) or living skin equivalents (Apligraf, Dermagraft) that are devices constructed from dermal cell types (fibroblasts, keratinocytes) grown on either natural (bovine collagen) or engineered matrixes producing sheets of engineered skin which can be applied to wounds after debridement.

In seeking a mechanistic hypothesis that could explain the differences between healing and nonhealing wounds, we were drawn to the role of proteases. Proteolysis in acute (healing) wounds is essential to enable migration of cells into the wound, to remodel granulation tissue, and to reform the architecture of normal dermis. However, excessive, inappropriate expression and activation of proteases occurs in chronic dermal ulcers, which is spatially and temporally aberrant.[5] Also, the levels of endogenous MMP inhibitors (TIMPs,

* To whom correspondence should be addressed. Tel +44 1304 649175; fax +44 1304 651987; e-mail jonathan_fray@sandwich.pfizer.com.
† Department of Discovery Chemistry.
‡ Department of Discovery Biology.
§ Current address: Renovo Ltd., The Manchester Incubator Building, 48 Grafton St., Manchester, M13 9XX, U.K.

10.1021/jm0308038 CCC: $25.00
Published on Web 07/04/2003

tissue inhibitors of metalloproteases) are reduced.[5] While TIMP-3 is abundantly expressed in both acute and chronic wounds, TIMP-1 can be found near the basement membrane in acute, but not in chronic, wounds, suggesting that the balance between MMPs and their inhibitors may be altered in poorly healing wounds.[6]

Three pathways explain why the proteolytic environment of chronic dermal ulcers is responsible for its pathology. First, while growth factors in fluids from chronic dermal ulcers (as measured using immunological assays) are present in comparable concentrations to those seen in acute wound fluids,[7] they lack biological activity[8] because they have been degraded.[7] Second, in chronic dermal ulcers, the receptors for growth factors are inactive due to proteolysis.[7] Last, in healing ulcers, fibroblasts migrate across a 'provisional matrix' and then deposit full granulation tissue after invasion of the wound. In chronic dermal ulcers, this matrix is degraded by the proteolytic environment which both prevents healing and causes ulcer autolysis. The limited efficacy of growth factors and artificial skin patches is probably due to their degradation by wound fluid.

Fibronectin is a key component of provisional matrix. Fibroblasts isolated from chronic dermal ulcers retain a normal ability to synthesize fibronectin,[9] while fluids from chronic dermal ulcers contained fibronectin fragments[10] and these fluids affected cells in a way compatible with matrix degradation.[11]

Fibronectin is a good substrate for Matrix metalloprotease-3 (MMP-3, stromelysin-1),[12] and MMP activity (MMP-3 in particular) has been shown to be up-regulated in chronic dermal ulcers.[6,13−17] It is of note that MMP activity is reduced in patients whose ulcers are entering a healing phase.[13] These data indicate that proteolysis of fibronectin is a key component of chronicity.

MMP-3 is known to degrade α1-anti-trypsin,[18] an endogenous inhibitor of neutrophil elastase, leading to reduced levels in chronic dermal ulcers.[19] Neutrophil elastase also degrades fibronectin but is expressed in highly variable amounts in patients with chronic dermal ulcers.[20] Hence, an MMP-3 inhibitor would also be expected to reduce the elastase activity which contributes to matrix degradation in some patients. α1-Antitrypsin also inhibits uPA (urokinase-type plasminogen activator),[21] thus its loss can potentiate uPA and hence the highly destructive enzyme, plasmin.

Thus, an inhibitor of MMP-3 would be expected to convert the environment of chronic dermal ulcers into that of acute wounds, enabling normal processes of healing to operate. There is some evidence to implicate MMP-3 activity in the healing of excisional but not incisional wounds.[22] In MMP-3 knockout mice the healing of excisional wounds was delayed compared to wounds in wild-type mice by disrupting the organization of fibroblasts that mediate early wound contraction.[22] The relevance of this finding to human chronic wounds is not clear, since wound contraction is a much more important process in rodents than humans.

MMP-3 is one of a family (sometimes called the matrixins) of structurally related zinc-containing metalloproteases that now number over 25 members.[23] Although other MMPs are to be found in chronic wound fluid, their presence is thought to be required only for

Chart 1[a]

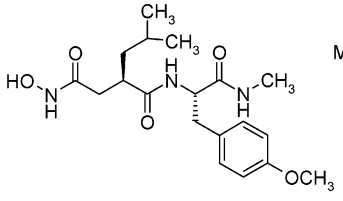

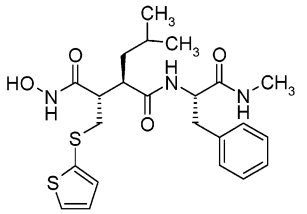

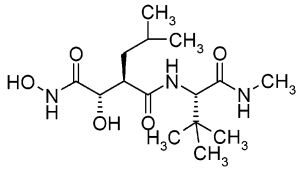

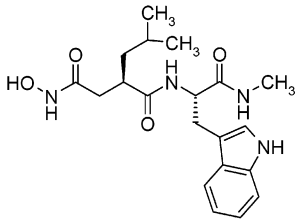

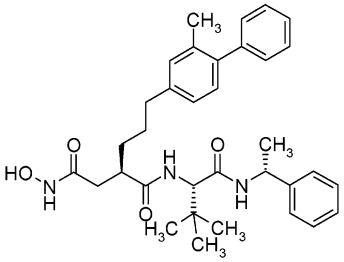

[a] (3*R*)-5-Methyl-3-{[(1*S*)-1-(methylcarbamoyl)-2-(4-methoxy)-phenylethyl]carbamoyl}hexanohydroxamic acid. [b]Data from ref 23. [c](2*S*,3*R*)-5-Methyl-3-{[(1S)-1-(methylcarbamoyl)-2-phenylethyl]carbamoyl}-2-[(2-thienylthio)methyl]hexanohydroxamic acid. [d](2*S*,3*R*)-*N*1-[(1*S*)-2,2-Dimethyl-1-(methylcarbamoyl)propyl]-(*N*4,2-dihydroxy)-5-methylbutanediamide. [e](2*R*)-*N*4-Hydroxy-*N*1-[(1*S*)-1-(1*H*-indol-3-ylmethyl)-2-(methylamino)-2-oxoethyl]-2-(2-methylpropyl)butanediamide. [f](2*R*)-*N*1-[(1*S*)-2,2-Dimethyl-1-({[(1*S*)-1-phenylethyl]amino}carbonyl)propyl]-2-{3-[(3-methyl-4-phenyl)-phenyl]propyl}-(*N*4-hydroxy)butanediamide.

wound healing. Thus, MMP-1 (fibroblast collagenase) is expressed by migrating keratinocytes at the wound edges.[24] There is evidence which suggests MMP-1 is required for keratinocyte migration on a collagen type I matrix in vitro and is completely inhibited by the presence of the nonselective MMP inhibitor SC44463 (**1**, Chart 1).[25] Keratinocyte migration in vivo is essential for effective wound healing to occur.

MMP-2 (gelatinase A, 72 kDa gelatinase) and MMP-9 (gelatinase B, 92 kDa gelatinase) appear to play important roles in wound healing during the extended re-

modeling phase and the onset of re-epithelialization, respectively.[26,27] The potent, nonselective MMP inhibitor BB-94 (batimastat, **2**, Chart 1) inhibits endothelial cell invasion of basement membrane, thereby inhibiting angiogenesis.[28] There is evidence that this process requires active MMP-2 and/or -9. Chronic wound fibroblasts have been shown to be unable to reorganize extracellular matrix and to lack active MMP-2 compared with normal dermal fibroblasts from the same patient.[29] Recently, studies have shown reduced MMP-2 production is associated with impaired dermal wound healing in genetically modified mice.[30]

MMP-14 (membrane-type-1 MMP, MT1-MMP) is responsible for the activation of MMP-2,[31] and thus inhibition of MMP-14 might indirectly affect the MMP-2 dependent processes described above.

MMP-13 (collagenase-3) is not present in acute wounds, nor in the epidermis of chronic dermal ulcers, but can be found in fibroblasts deep in the chronic ulcer bed, where its role may be to remodel collagenous matrix.[32]

Thus, nonselective MMP inhibitors that inhibit MMPs 1, 2, 9, or 14 would be expected to impair wound healing, whereas inhibition of MMP-3 and MMP-13 should allow chronic wounds to revert to a pattern of normal healing.

Reports of the effects of nonselective MMP inhibitors on wound healing are rather scant. In an in vitro model of one of the stages of wound healing, the potent, nonselective MMP inhibitor marimastat (BB-2516, **3**, Chart 1) was found to inhibit fibroblast-mediated collagen lattice contraction indicating that MMPs play an important role in the contraction of granulation tissue.[33] However, in the case of sutured wounds where the wound edges are brought together, marimastat was without effect.[34] The MMP-1-sparing MMP inhibitor BB-3103 prevented epithelialization in a cultured human skin explant model, thereby implicating the requirement for active MMP-2.[35]

These reports are supported by in vivo evidence in a study of healing of partial thickness dermal wounds in pigs.[36] The broad spectrum MMP-inhibitor, GM-6001 (ilomastat, **4**, Chart 1), applied topically almost completely inhibited all MMP activity, and this was associated with a significant reduction in epithelial coverage compared with controls, although inflammatory responses and epithelial proliferation were unaffected. GM-6001 has also been found to delay healing of human blister wounds in vivo.[37]

We also required selectivity over certain other zinc-dependent enzymes, less closely related to MMP-3.[38] One of these is pro-collagen C-proteinase (PCP)[39] which is released by dermal fibroblasts and which is required during normal wound healing to convert pro-collagen into its insoluble form prior to further transformation into a cross-linked matrix. Another is TACE (tumor necrosis factor-α converting enzyme) that is responsible for the release of the cytokine TNF-α.

Our approach to the design of selective MMP-3 inhibitors has recently been described.[40,41] In a series of succinyl hydroxamic acid derivatives, we discovered that subtle modifications to both P1′ and P3′ groups led to increased inhibitory potency against MMP-3 while diminishing inhibition of MMP-1, -2, -9, and -14. The most selective compound was UK-356,618 (**5**, Chart 1) (MMP-3 IC_{50} = 5.9 nM, selectivity ≥ 140-fold vs MMP-1, -2, -9, and -14), which possessed sufficient potency and selectivity in vitro to be considered for further progression for the topical treatment of chronic wounds. We intended to use a topical approach for several reasons. First, succinyl hydroxamic acids (and their carboxylic acid derivatives) were known to possess very poor pharmacokinetic properties (high clearance, low oral absorption), and topical administration would be an obvious way to overcome these deficiencies through easy access to the site of action. Chronic dermal wounds have limited vascularization that might hamper the ability of a systemically available agent to reach the wound site. Furthermore, since selectivity was of prime concern, it would be advantageous to have high local but low systemic drug concentrations. Joint pain has been experienced by patients during clinical trials of orally active, nonselective, and MMP-1-sparing MMP inhibitors,[42] that may be related to the broad spectrum zinc protease inhibitory activity of these compounds. Topical administration might avoid this side effect. The amount of drug entering the wound would also be limited by the size of the wound. However, **5** was deemed unsuitable for development because it possessed limited chemical stability. Results from accelerated degradation studies predicted a suitable shelf life in an aqueous-based vehicle (2-years at room temperature), but insufficient stability for the production of a sterile formulation (necessary for application to an open wound). Furthermore, **5** could only be obtained as an amorphous, low-melting solid and so a crystalline physical form could not be defined.

While examining the structure−activity relationships of a number of close analogues of **5**, we prepared the *O*-methylphenylglycinol derivative **6**, since this P3′ group had been shown to be slightly superior to α-methylbenzylamine in previous studies.[40] This compound had comparable potency and selectivity to **5**, but suffered from the same lack of crystallinity. The related carboxylic acid **7** was prepared as an intermediate and profiled in our in vitro enzyme inhibition assays. To our surprise, compound **7** was unusually potent compared to previous carboxylic acid derivatives (which had IC_{50} ≥ 100 nM vs MMP-3) and even more selective than **5** or **6**. In common with other carboxylic acids we had made, it was readily crystallized and was significantly more stable toward chemical degradation; thus, it was a superior choice for progression as a development candidate. This paper describes the synthesis, in vitro profile, topical and systemic pharmacokinetics of **7**, and demonstration of inhibition of MMP-3 in vivo in a model of chronic dermal wounds.

Chemistry

The synthesis of **7** was based on the method of Plattner et al.,[43] first used for the synthesis of renin inhibitors, in which the homochiral succinic acid half ester **13** is constructed via alkylation of an Evans chiral acyloxazolidinone.[44] The succinic acid half ester **13** and a homochiral amine dipeptide mimic **16** were then brought together in a standard peptide coupling reaction followed by deprotection of the resulting *tert*-butyl ester **17** (Scheme 1).

The preparation of **13** required the bromobiphenyl derivative **9**. Although this could be prepared by a

Scheme 1[a]

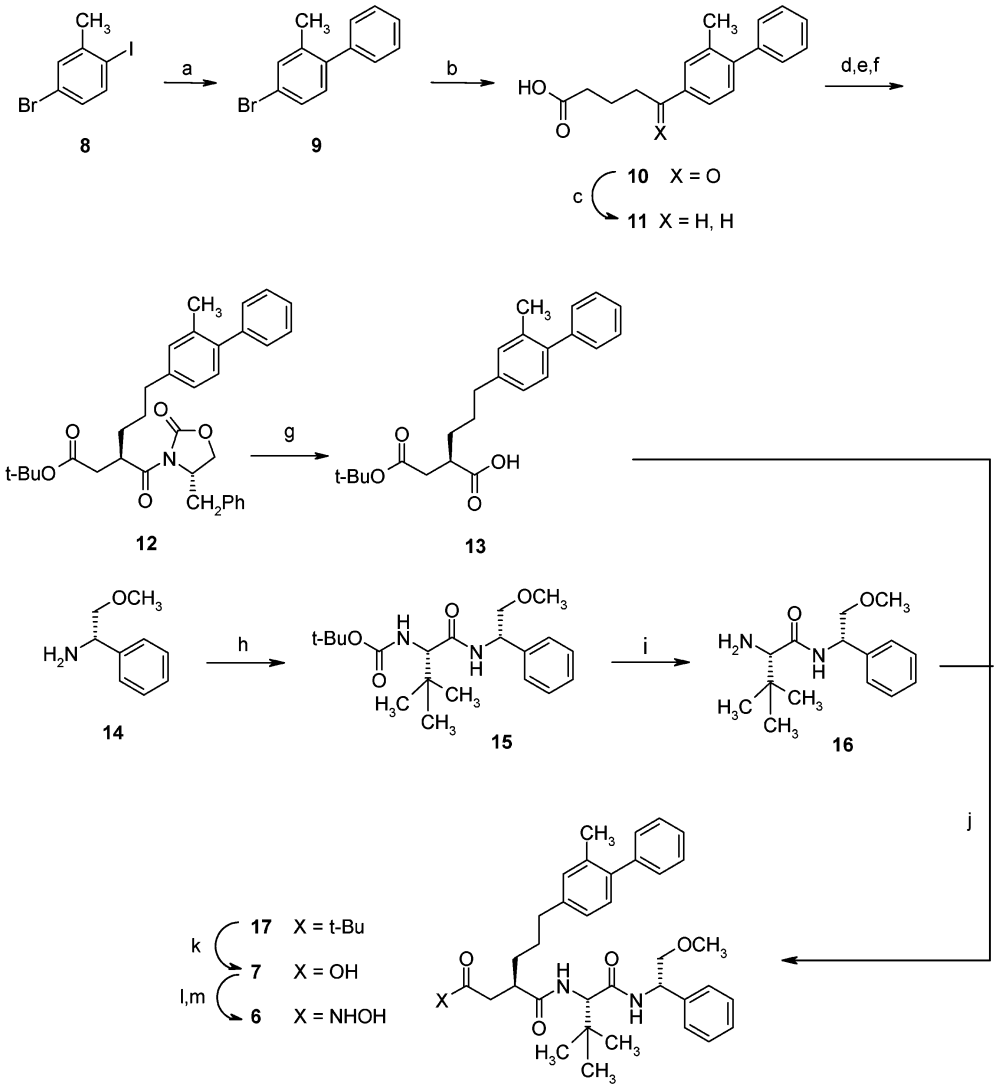

[a] (a) $PhB(OH)_2$, cat. $Pd(OAc)_2/PPh_3$, 2 M Na_2CO_3, H_2O/acetone, reflux; (b) Mg, THF, reflux, then glutaric anhydride, THF, −40 °C; (c) Et_3SiH, CF_3CO_2H, 20 °C; (d) $(COCl)_2$, CH_2Cl_2, cat. DMF, 20 °C; (e) 4-(*S*)-benzyloxazolidin-2-one, n-BuLi, THF, −70 °C; (f) $NaN(SiMe_3)_2$, THF, −70 °C, then $BrCH_2CO_2Bu^t$; (g) LiOH, H_2O_2, THF/H_2O; (h) *N*-Boc-*tert*-leucine, EDC, HOBt, NMP, 2−20 °C; (i) $HCl_{(g)}$, CH_2Cl_2/dioxane, 4−20 °C; (j) EDC, HOBt, $EtN(Pr^i)_2$, 4−20 °C; (k) CF_3CO_2H/CH_2Cl_2 = 1:1, 20 °C; (l) *O*-allylhydroxylamine, PyAOP, $EtN(Pr^i)_2$, 0−20 °C; (m) NH_4^+ HCO_2^-, cat. $Pd(OAc)_2/PPh_3$, EtOH/H_2O, reflux.

Gomberg−Bachmann−Hey reaction[45] (4-bromo-2-methylaniline, isoamyl nitrite, benzene, reflux) the yield was modest (≤40%). Subsequently, we discovered that chemoselective Suzuki reaction between 5-bromo-2-iodotoluene (**8**) and phenylboronic acid proceeded much more cleanly to afford **7** in 79% yield. Attachment of the pentanoic acid chain was achieved via generation of the Grignard reagent from **9** and reaction with glutaric anhydride,[46] followed by reduction of the ketone (**10**) with triethylsilane/trifluoroacetic acid[47] to give **11** (48% from **9**). Elaboration of **11** to give **13** took four steps; conversion to the acid chloride, attachment of the Evans benzyl oxazolidinone chiral auxiliary, diastereoselective alkylation using sodium hexamethyldisilazide as base and *tert*-butyl bromoacetate as the electrophile, and finally cleavage of the chiral auxiliary (overall yield 52%).

Amine **16** was readily prepared from (*S*)-*O*-methylphenylglycinol (**14**)[48] by coupling with (*S*)-*N*-Boc-*tert*-leucine[49] and removal of the Boc group from **15**. Coupling of **13** to **16** under standard conditions (EDC, HOBt, CH_2Cl_2, 0−20 °C) proceeded in quantitative yield. Removal of the *tert*-butyl ester was achieved using 50% trifluoroacetic acid in dichloromethane to afford **7** as a colorless solid that was readily recrystallized from hot ethyl acetate. Hydroxamic acid **6** was prepared in two steps from **7** using the method previously described.[40]

Results and Discussion

The in vitro enzyme inhibition profile of compound **7** will be discussed in comparison with that of compounds **2**, **5**, and **6** (Table 1). The assays involved catalytic domains of human recombinant MMPs (MMP-1, -2, -3, -9, -13, and -14) and measured the concentration of inhibitors that were able to prevent cleavage of fluorogenic peptide substrates. Full details are given in the Experimental Section.

Compound **2** is typical of nonselective succinyl hydroxamate MMP inhibitors. It possesses small alkyl groups at P1′ (i.e., isobutyl) and P3′ (methyl) that fit well into the binding sites of all MMPs. The high inhibitory potency (≤5 nM) is presumably driven by the

Table 1. Enzyme Inhibition Profile of Compounds **2**−**5** and **14** (data are IC_{50} (nM) (SEM (*n*))

	compound			
enzyme	**2**	**5**	**6**	**7**
MMP-1	0.99 ± 0.34 (5)	51000 ± 27000 (4)[a]	5900 (1)	20% inhibition at 100 μM (5)
MMP-2	0.73 ± 0.07 (5)	1790 ± 1000 (5)[a]	750 (1)	34200 ± 17800 (9)
MMP-3	0.56 ± 0.06 (5)	5.9 ± 2.2 (5)[a]	2.1 (1)	23 ± 9 (12)
MMP-9	0.60 ± 0.11 (5)	840 ± 91 (5)[a]	560 (1)	30400 ± 13400 (9)
MMP-13	5.0 ± 1.3 (3)	73 ± 1.4 (4)[a]	NT	2300 (2)
MMP-14	4.6 ± 1.2 (5)	1900 ± 450 (4)[a]	930 (1)	66900 ± 11700 (10)
PCP[c]	NT[b]	52000 (2)	NT	14% inhibition at 100 μM ± 12% (3)
TACE[d]	14.9 ± 5.6 (11)	NT	NT	17% inhibition at 100 μM (1)

[a] Data from ref 41. [b] NT = not tested. [c] PCP = pro-collagen C-proteinase. [d] TACE = TNFα converting enzyme.

hydroxamate binding to the catalytic zinc atom in a bidentate manner and by a network of hydrogen bonds between the hydroxamate and two trans amidic linkages to the enzymes' substrate binding groove. The profile of compound **5** has already been described.[41] By introducing both a bulky branched P3′ group (α-methylbenzyl) of the correct configuration and an ortho-substituted biphenpropyl group at P1′, substantial selectivity (≥140-fold) was achieved. Compound **6**, which is also a hydroxamate, has a very similar enzyme inhibition profile to compound **3**. The only difference in the structures is a slight modification to P3′, where an *O*-methylphenylglycinol replaces the α-methylbenzyl. The result is a slight increase (ca. 2-fold) in potency vs MMP-2, -3, -9, and -14 with no significant change in selectivity. Compound **7**, as is typical of carboxylic acid inhibitors, is less potent than the corresponding hydroxamate **6** (about 10-fold vs MMP-3) but is somewhat more selective (≥1200-fold vs MMPs 1, 2, 9, and 14). We attribute this profile to the fact that the carboxylic acid is a weaker zinc ligand than hydroxamate, and although this causes a diminution in potency overall, it permits a much greater proportion of the binding energy to be derived from the hydrophobic groups. It is the structure of these and the way they interact with the various MMP binding sites that determines selectivity for one MMP over another, since the zinc binding group and trans,trans diamide hydrogen bonding groups are the same for all the other compounds discussed here.

The potency of compound **7** for the inhibition of MMP-13 was determined to be 2.3 μM, some 100-fold less potent than its inhibition of MMP-3. It is thus likely that compound **7** would be ineffective at inhibiting MMP-13 in in vivo situations. However, although MMP-13 has been shown to be present in chronic but not acute wounds, its contribution to the pathology of chronic wounds is not established. Compound **7** was found to be inactive (IC_{50} > 100 μM) vs zinc metalloproteases PCP and TACE and possessed the following inhibitory potencies vs MMP-7 (IC_{50} = 5.8 μM), MMP-8 (IC_{50} = 1.75 μM), and MMP-12 (IC_{50} = 42 nM). The latter three MMPs do not appear to have a role in wound healing, at least up to the completion of re-epithelialization, at which point penetration of compound **7** into the wound site would probably by inhibited by the new epidermis.

The inhibition potency of **7** against MMP-3, -2, and -9 was also measured using radiolabeled natural substrates. Thus, compound **7** potently inhibited cleavage of [^{3}H]-fibronectin by MMP-3 (IC_{50} = 320 ± 90 nM, *n* = 3) but did not inhibit cleavage of [^{3}H]-gelatin by either MMP-2 or -9 up to the highest concentration tested (100 μM). The 14-fold lower potency for inhibition of MMP-3 when fibronectin was the substrate may be due to higher protein binding by compound **7** in the assay. Compound **2** also showed a similar fall in potency in the MMP-3 (fibronectin) assay (IC_{50} =13.9 ± 4.6 nM, *n* = 3).

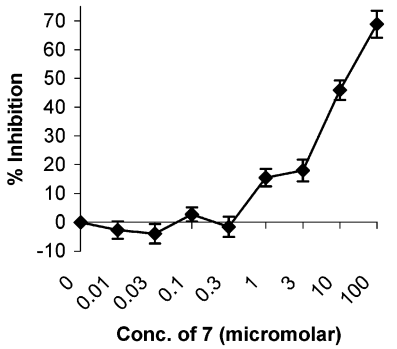

Figure 1. Effects of Compound **7** on Keratinocyte Migration over Collagen Type I (*n* = 3).

Table 2. Effect of Varying Concentrations of Compound **7** on Keratinocyte Migration over a Collagen Matrix (*n* = 3)

concentration of compound **7** (μM)	mean % inhibition of migration	SEM
vehicle	0	
0.01	−2.7	3.0
0.03	−4.0	3.4
0.1	2.7	2.5
0.3	−1.6	3.5
1	15.5	3.0
3	18.0	3.8
10	45.9	3.4
100	68.8	4.7

The functional selectivity of compound **7** in vitro was demonstrated by examining its effect on keratinocytes migrating over a collagen matrix which requires active MMP-1, -2, and -9.[25,37,50,51] Compound **7** inhibited this process, as shown in Figure 1 and Table 2, only at concentrations consistent with its potency vs MMPs-2 and -9 (see above) and greatly in excess of that needed to inhibit MMP-3. Furthermore, compound **7** was not cytotoxic to, nor affected proliferation of, fibroblasts, keratinocytes, or endothelial cells at 50−100 μM in vitro.

Having established that compound **7** had the desired potency and selectivity profile in vitro, we next examined its pharmacokinetic properties following iv administration to rats (2 mg/kg, *n* = 3). As expected for a high molecular weight, lipophilic carboxylic acid, compound **7** possessed high clearance with respect to liver blood flow (88 mL/min/kg) and moderate volume of distribution (3.1 L/kg) resulting in a short elimination phase ($t_{1/2}$ = 23 min). Following oral administration (50

Table 3. Inhibition of MMP-3 by Compound **7** in Rabbit Adriamycin Wounds Ex Vivo, Corresponding Drug Concentrations, and in Vitro Potency for Inhibition of [^{3}H]-Fibronectin Cleavage

		drug concentration (μM)				
		top of wound		bottom of wound		fibronectin cleavage IC_{50} (μM) (in vitro)
dosing regimen	% inhibition of MMP-3	total	free[a]	total	free[a]	
high	79 ± 6[b] ($n = 6$)	4421[c]	26.52	549[d]	3.29	0.32 ± 0.09
low	47 ± 11 ($n = 7$)	966[e]	5.79	65[f]	0.39	

[a] Estimated free concentration calculated from the total drug concentration, assuming tissue binding was equal to protein binding of **7** (99.4%) in rabbit plasma. [b] $p < 0.005$. [c] Mean of $n = 8$. [d] Mean of $n = 6$. [e] Mean of $n = 7$. [d] Mean of $n = 4$.

mg/kg), bioavailability was very low (<5%). The absorption following oral dosing of similar, high molecular weight carboxylic acid MMP inhibitors has also been reported to be very low.[52−54] These data supported our strategy to develop a topically administered compound, since this would be the only way to achieve sufficient exposure in the wound, but yet minimize systemic exposure.

To measure pharmacokinetic parameters following topical dermal administration, we chose to use a model of chronic wounds in which intradermal adriamycin injections in rabbits were used to induce wounds modeling certain features of chronic wounds in man.[55] Whereas normal dermal wound healing in rabbits is essentially complete within 10 days, the adriamycin-induced wounds exhibit a chronic nonhealing period up to 28 days postinjection, which is associated with elevated levels of MMP-3 (but not MMP-2 or -9) within the wound. Eventually, MMP-3 levels subside and the wounds enter the healing phase, which is typically complete by day 49. This healing phase is characterized by a lack of MMP-3 expression and elevated levels of MMP-2/9.

Using this model we measured both the wound pharmacokinetics of compound **7** and its ability to inhibit MMP-3 (day 7 to 13). Preliminary pharmacokinetic studies using topical application as a suspension in hydrogel established that the clearance rate from wound tissue was found to be slow with a half-life of ca. 3 days and permitted us to design a suitable dosing regimen for the pharmacodynamic study. This comprised a 'high' dose regimen, in which an initial dose of 15 mg/wound on day 7 was followed by a further dose (7.5 mg/wound) on day 10. On day 13, wound tissue was harvested and analyzed for concentrations of compound **7** present and inhibition of MMP-3. Similarly, a 'low' dose regimen was also employed (5 mg/wound on day 7, followed by 2.5 mg/mL on day 10, wounds harvested day 13). Under neither dosing regimen was any compound **7** found in plasma samples (limit of detection 17 nM). To analyze for compound **7**, tissue slices were extracted with an organic solvent and compound concentrations determined by quantitative HPLC. To determine the inhibition of MMP-3, tissue slices were incubated in the presence of the specific fluorogenic MMP-3 substrate Mca-Arg-Pro-Lys-Pro-Val-Glu-Nva-Tyr-Arg-Lys(Dnp)NH_2. A commercially available cocktail of serine and cysteine protease inhibitors was added to prevent non-MMP mediated cleavage of the substrate, but despite this some was observed. We therefore determined the background substrate cleavage by adding 100 μM compound **2** to inhibit completely all MMPs present and used these data to define the upper limit of MMP inhibition. One of the limitations of the method to determine the inhibition of MMP-3 was that the tissue slices (ca. 0.25 μL in volume) had to be suspended in buffer (50 μL) prior to the addition of the specific MMP-3 substrate. Thus, it is likely that compound **7** would have been diluted into the buffer at least to some extent. In consequence, the extent of inhibition of MMP-3 achieved by the concentration of compound (where there was no dilution involved in the measurement of that concentration) is probably an underestimate.

The results of these experiments are shown in Table 3. Compound **7** showed a dose-dependent inhibition of MMP-3, with almost complete inhibition being achieved at the high dose. Under both dosing regimes, compound **7** was present in both top and bottom of the wound tissue in significant concentrations compared to that required to inhibit MMP-3-mediated fibronectin cleavage in vitro, i.e., estimated free drug concentrations ≥ 0.32 μM.

Conclusions

A large body of evidence has linked the pathology of human chronic dermal wounds to the overexpression and activity of MMP-3, which degrades fibronectin, a key constituent of extracellular matrix. Compound **7** is a potent inhibitor of MMP-3 with substantial selectivity (>1200-fold) over MMPs 1, 2, 9, and 14, whose activity must be preserved for normal wound healing to take place. MMP-13, which may also contribute to the pathology of chronic wounds, was inhibited some 100-fold less potently by compound **7**. Compound **7** had essentially no affinity for the related zinc metalloproteases PCP and TACE, and consequently it is unlikely to affect collagen production or inflammatory cell responses during wound healing.

We have demonstrated that compound **7** is able to inhibit MMP-3 in a model of chronic dermal wounds at concentrations that would be expected to spare MMP-2 and -9. In addition, it possesses physicochemical and pharmacokinetic properties (high protein binding, extended residence time in wound tissue, and rapid systemic clearance) that make it suitable for once-weekly topical administration to chronic dermal wounds, a dosing regime that is compatible with current nursing care. Although compound **7** was less potent than its related hydroxamic acid derivative **6**, it possesses better crystallinity and chemical stability.

These properties make compound **7** a suitable candidate for progression to clinical trials in human chronic dermal wounds, such as venous ulcers.

Experimental Section

Melting points were determined using open glass capillary tubes and a Gallenkamp melting point apparatus and are uncorrected. Nuclear magnetic resonance (NMR) data were

obtained using Varian Unity Inova-400, Varian Unity Inova-300, or Bruker AC300 spectrometers and are quoted in parts per million from tetramethylsilane. Mass spectral (MS) data were obtained on a Finnigan Mat. TSQ 7000 or a Fisons Instruments Trio 1000. The calculated and observed ions quoted refer to the isotopic composition of lowest mass. Infrared (IR) spectra were measured using a Nicolet Magna 550 Fourier transform infrared spectrometer. Combustion analyses were performed by Exeter Analytical, Uxbridge, U.K. Flash chromatography refers to column chromatography on silica gel (Kieselgel 60, 230−400 mesh), from E. Merck, Darmstadt. Kieselgel 60 F_{254} plates from E. Merck were used for TLC, and compounds were visualized using UV light, 5% aqueous potassium permanagate, or Dragendorff's reagent (oversprayed with aqueous sodium nitrite). Hexane refers to a mixture of hexanes (HPLC grade) bp 65−70 °C. Ether refers to diethyl ether.

1-Hydroxy-7-aza-1*H*-1,2,3-benzotriazole (HOAt) and 7-azabenzotriazol-1-yloxytris(pyrrolidino)phosphonium hexafluorophosphate (PyAOP) were purchased from PerSeptive Biosystems U.K. Ltd. 5-bromo-2-iodotoluene (**6**) was purchased from Wychem Ltd, Suffolk, U.K. (1*S*)-2-Methoxy-1-phenylethylamine (**11**) was prepared according to the literature method.[48] The specific MMP-3 substrate Mca-Arg-Pro-Lys-Pro-Val-Glu-Nva-Tyr-Arg-Lys(Dnp)NH_2[56] was purchased from Bachem.

Chemistry. 3-Methyl-4-phenylbromobenzene (9). A mixture of 5-bromo-2-iodotoluene (**8**) (5.01 g, 16.9 mmol), phenylboronic acid (2.26 g, 18.5 mmol), palladium acetate (190 mg, 0.85 mmol), triphenylphosphine (440 mg, 1.68 mmol), and 2 M aqueous sodium carbonate (25 mL) in acetone (60 mL) was degassed and heated at reflux under nitrogen for 18 h. The mixture was cooled and partitioned between ether (200 mL) and water (100 mL). The organic layer was washed with brine (100 mL), dried ($MgSO_4$), and concentrated under reduced pressure to give a yellow oil. Purification by flash chromatography (eluting with hexane) gave **9** (3.298 g, 79%) whose spectroscopic data were identical with a sample prepared by the literature method.[45]

5-(3-Methyl-4-phenylphenyl)-5-oxopentanoic Acid (10). A solution **9** (12.36 g, 50.0 mmol) in anhydrous tetrahydrofuran (30 mL) was added dropwise at reflux to a suspension of magnesium turnings (1.33 g, 50 mmol) in anhydrous tetrahydrofuran (23 mL) containing a crystal of iodine under nitrogen with mechanical stirring. After the addition was complete, the mixture was diluted with anhydrous tetrahydrofuran (55 mL) and heating continued for 1 h. The resulting solution was allowed to cool to room temperature and then added dropwise via syringe to a solution of glutaric anhydride (6.27 g, 55 mmol) in anhydrous tetrahydrofuran (125 mL) under nitrogen at −40 °C. After 90 min at −40 °C, the mixture was allowed to warm to 0 °C, and hydrochloric acid (1 M, 250 mL) was added. The mixture was extracted with ether (500 mL), washed with brine (200 mL), dried ($MgSO_4$), and concentrated under reduced pressure. The residue was purified by flash chromatography (eluting with dichoromethane:methanol = 95:5) to give **10** as a pale brown oil, (8.6 g, 60%) which subsequently crystallized. mp 91−94 °C. Anal. (C, H). R_f 0.26 (dichoromethane:methanol = 95:5). δ_H (400 MHz, $CDCl_3$) 2.11 (2H, pentet, J = 7 Hz), 2.33 (3H, s), 2.50 (2H, t, J = 7 Hz), 3.11 (2H, t, J = 7 Hz), 7.31 (3H, m), 7.42 (3H, m), 7.84 (1H, d, J = 8 Hz), 7.90 (1H, s). LRMS (thermospray) m/z = 283 (MH^+).

5-(3-Methyl-4-phenylphenyl)pentanoic Acid (11). To a stirred solution of **10** (1.0 g, 3.5 mmol) in trifluoroacetic acid (5 mL) under nitrogen at 0 °C was added triethylsilane (1.4 mL, 8.75 mmol) dropwise over 2 min. The mixture was then allowed to warm to room temperature and stirred for 2 h. The mixture was poured into water (20 mL) and extracted with dichloromethane (3 × 15 mL). The combined organic solutions were washed with brine, dried ($MgSO_4$), and concentrated under reduced pressure. The mixture was purified by flash chromatography (eluting with dichloromethane:methanol = 95:5) to give a 3:1 mixture of **11** and triethylsilanol (1.1 g). This material was dissolved in hexane (5 mL), and sodium hydrogen carbonate (290 mg, 3.5 mmol) was added. The mixture was stirred overnight at room temperature and then concentrated under reduced pressure. The solid residue was triturated with ethyl acetate and filtered to give **11** (sodium salt) (820 mg, 80%). Treatment of this material with hydrochloric acid and solvent extraction gave **11** as a viscous, colorless gum. Anal. (C, H). δ_H (400 MHz, $CDCl_3$) 1.74 (4H, m), 2.27 (3H, s), 2.43 (2H, m), 2.65 (2H, m), 7.06 (1H, d, J = 8 Hz), 7.11 (1H, s), 7.16 (1H, d, J = 8 Hz), 7.33 (3H, m), 7.42 (2H, m). LRMS (thermospray) m/z = 286 (MNH_4^+).

***tert*-Butyl (3*R*)-3-[(4-(*S*)-4-Benzyl-2-oxo-1,3-oxazolidin-3-yl)carbonyl]-6-(3-methyl-4-phenylphenyl)hexanoate (12).** (a) Oxalyl chloride (3.1 mL, 35.5 mmol) was added dropwise to a stirred solution of **11** (6.80 g, 25.3 mmol) in anhydrous dichloromethane (60 mL) under nitrogen at −10 °C. Dimethylformamide (2 drops) was added, and after 10 min, the mixture was allowed to warm to room temperature. After 5 h, the solution was concentrated under reduced pressure, and the residue dissolved in anhydrous toluene and concentrated under reduced pressure (twice). The residue was dissolved in hexane (150 mL), allowed to stand for 17 h, and then filtered through Arbocel filter aid, washing the filter cake with more hexane. The filtrate was concentrated under reduced pressure to give 5-(3-methyl-4-phenylphenyl)pentanoyl chloride (7.1 g, 97%), as a pale yellow oil, which was used directly for the next reaction without purification. δ_H (400 MHz, $CDCl_3$) 1.77 (4H, m), 2.26 (3H, s), 2.63 (2H, t, J = 6.5 Hz), 2.95 (2H, t, J = 6.5 Hz), 7.06 (1H, d, J = 8 Hz), 7.10 (1H, s), 7.36 (5H, m).

b) A solution of *n*-butyllithium (9.92 mL, 2.5 M in hexanes, 24.8 mmol) was added dropwise over 15 min to a solution of 4-(*S*)-benzyloxazolidin-2-one (4.39 g, 24.8 mmol) in anhydrous tetrahydrofuran (70 mL) under nitrogen at −70 °C. The mixture was allowed to warm to −50 °C for 30 min and then recooled to −70 °C. A solution of 5-(3-methyl-4-phenylphenyl)-pentanoyl chloride (7.1 g, 24.8 mmol) in anhydrous tetrahydrofuran (10 mL) was added dropwise over 15 min. After 1 h, the mixture was allowed to warm to 0 °C whereupon 20% aqueous ammonium chloride (75 mL) was added rapidly. After being stirred for 15 min, the mixture was extracted with ethyl acetate (250 mL), and the organic phase washed with water (3 × 250 mL), dried ($MgSO_4$), and concentrated under reduced pressure. The residue was purified by flash chromatography (gradient elution with pentane:ethyl acetate = 20:1 to 2:1) to give 4-(*S*)-benzyl-3-{5-(3-methyl-4-phenylphenyl)pentanoyl}-oxazolidin-2-one (9.66 g, 91%) as a colorless oil. R_f 0.4 (pentane: ethyl acetate = 3:1). Anal. (C, H, N). δ_H (300 MHz, $CDCl_3$) 1.79 (4H, m), 2.28 (3H, s), 2.70 (2H, m), 2.79 (1H, dd, J = 10 and 13 Hz), 3.01 (2H, m), 3.32 (1H, dd, J = 3 and 13 Hz), 4.19 (2H, m), 4.70 (1H, m), 7.06−7.43 (13H, complex). LRMS (thermospray) m/z = 445 (MNH_4^+). FTIR (KBr disk) 2930, 1784, 1700, 1387, 1350, 1211, 702 cm^{-1}.

(c)A solution of sodium hexamethyldisilazide (31.3 mL, 1 M in tetrahydrofuran, 31.3 mmol) was added dropwise over 30 min to a stirred solution of 4-(*S*)-benzyl-3-{5-(3-methyl-4-phenylphenyl)pentanoyl}oxazolidin-2-one (13.39 g, 31.3 mmol) in anhydrous tetrahydrofuran (100 mL) at −75 °C. After 1 h, a solution of *tert*-butyl bromoacetate (4.95 mL, 33.5 mmol) in anhydrous tetrahydrofuran (10 mL) was added dropwise over 20 min, keeping the temperature below −70 °C. The mixture was stirred at this temperature for 2 h and then allowed to warm to −50 °C at which point 20% aqueous ammonium chloride (150 mL) was added with rapid stirring. The mixture was allowed to warm to 10 °C and then poured into a mixture of ethyl acetate (400 mL) and water (200 mL). The organic phase was separated, washed with water (3 × 250 mL), dried ($MgSO_4$), and concentrated under reduced pressure. The residue was purified by flash chromatography (gradient elution with pentane:ether = 20:1 to 1:1) to give **12** as a colorless oil (10.4 g, 61%). Anal. (C, H, N).

R_f 0.6 (pentane:ether = 1:1). δ_H (300 MHz, $CDCl_3$) 1.45 (9H, s), 1.58 (1H, m), 1.74 (3H, m), 2.27 (3H, s), 2.51 (1H, dd, J = 5 and 18 Hz), 2.65 (2H, m), 2.80 (2H, m), 3.38 (1H, dd, J = 3 and 15 Hz), 4.16 (2H, d, J = 5 Hz), 4.25 (1H, m), 4.68 (1H, m), 7.04 (1H, d, J = 8 Hz), 7.08 (1H, s), 7.14 (1H, d, J = 8 Hz), 7.35 (10H, complex). LRMS (thermospray) m/z = 542 (MH^+),

560 (MNH_4^+). FTIR $\nu_{max.}$ (KBr disk) 2980, 2930, 1780, 1725, 1700, 1388, 1350, 1157, 768, 702 cm^{-1}.

***tert*-Butyl (3*R*)-3-(Carboxy)-6-(3-methyl-4-phenylphenyl)hexanoate (13).** 30% Aqueous hydrogen peroxide (12.75 mL, 114 mmol) was added dropwise to a solution of **12** (10.3 g, 19.0 mmol) in tetrahydrofuran:water (3:1, 400 mL) at 0 °C. Then lithium hydroxide monohydrate (1.595 g, 38.0 mmol) was added in one portion. The mixture was stirred for 2 h at 0 °C and 1 h at 20 °C. The reaction mixture was recooled to 0 °C, and a solution of sodium sulfite (15.56 g, 123.5 mmol) in water (80 mL) was added dropwise over 15 min. The mixture was stirred rapidly at 0 °C for 2.5 h, and then 2 M hydrochloric acid (ca. 8 mL) was added to adjust the pH to 6. The mixture was concentrated under reduced pressure to half volume, acidfied to pH 2 by the addition of 2 M hydrochloric acid, and extracted with dichloromethane (400 mL and 2 × 200 mL). The combined extracts were dried ($MgSO_4$) and concentrated under reduced pressure, and the residue was purified by flash chromatography (gradient elution with pentane:ether = 15:1 to 1:4) to give **13** (7.05 g, 97%) as a colorless oil. $[\alpha]_D = +12.9°$ (c = 0.716, methanol, 25 °C). Anal. (C, H). R_f 0.5 (pentane: ether:acetic acid = 30:70:1). δ_H (300 MHz, $CDCl_3$) 1.45 (9H, s), 1.63 (1H, m), 1.77 (4H, m), 2.26 (3H, m), 2.42 (dd, J = 5 and 17 Hz), 2.65 (3H, m), 2.87 (1H, m), 7.06 (2H, m), 7.15 (1H, d, J = 8 Hz), 7.34 (5H, m). LRMS (thermospray) m/z = 400 (MNH_4^+). FTIR $\nu_{max.}$(film) 2980, 2930, 1730, 1705, 1485, 1368, 1157, 764, 702 cm^{-1}.

(2*S*)-*tert*-(Butoxycarbonyl)amino-3,3-dimethyl-*N*-[(1*S*)-2-methoxy-1-phenylethyl]butanamide. *N*-(Dimethylaminopropyl)-*N*′-ethylcarbodiimide hydrochloride (25.35 g, 132.3 mmol) was added to a stirred mixture of *tert*-butyl *N*-[(1*S*)-2,2-dimethyl-1-carboxypropyl]carbamate (27.79 g, 120.3 mmol), (1*S*)-2-methoxy-1-phenylethylamine (**14**) (19.12 g, 126.6 mmol), *N*-methylmorpholine (14.4 mL, 132.3 mmol), and 1-hydroxy-1,2,3-benzotriazole hydrate (20.24 g, mmol) in anhydrous dichloromethane (600 mL) under nitrogen at 2 °C. The mixture became homogeneous after 10 min. The mixture was stirred for 1 h and then allowed to warm to room temperature. After 2.5 h at room temperature, the mixture was concentrated under reduced pressure, and the residue was diluted with ethyl acetate (1400 mL), washed sequentially with 5% aqueous citric acid (2 × 500 mL), saturated aqueous sodium bicarbonate (2 × 250 mL), and brine (250 mL), dried ($MgSO_4$), and concentrated under reduced pressure. The residue was recrystallized from hot ethyl acetate/hexane (1:2, 300 mL) to give the title compound (20.02 g, 46%), as a colorless solid, mp 135−137 °C. Anal. (C, H, N). δ_H (400 MHz, $CDCl_3$) 1.03 (9H, s), 1.44 (9H, s), 3.35 (3H, s), 3.63 (2H, d, J 7 Hz), 3.85 (1H, d, J 10 Hz), 5.13 (1H, q, J 7 Hz), 5.20 (1H, br d, J 10 Hz), 6.34 (1H, br d, J 10 Hz), 7.30 (5H, m). LRMS (thermospray) m/z = 365 (MH^+), FTIR $\nu_{max.}$ (KBr disk) 3290, 2973, 1721, 1685, 1633, 1173, 702 cm^{-1}. The mother liquors were concentrated under reduced pressure, and the residue was triturated with ether to afford an additional 15.44 g (35%) of product.

(2*S*)-Amino-3,3-dimethyl-*N*-[(1*S*)-2-methoxy-1-phenylethyl]butanamide Hydrochloride (16). (2*S*)-*tert*-(Butoxycarbonyl)amino-3,3-dimethyl-*N*-[(1*S*)-2-methoxy-1-phenylethyl]-butanamide (34.99 g, 96.0 mmol) was dissolved in a mixture of anhydrous dichloromethane (250 mL) and dioxane (250 mL) and cooled to 2 °C. Hydrogen chloride gas was bubbled through the solution with stirring until a saturated solution had formed (about 1 h). After being stirred for 40 min at 4 °C, the solution was warmed to room temperature and stirred for an additional 40 min. The solution was concentrated under reduced pressure. The residue was slurried with anhydrous ether (200 mL) and evaporated (three times), and the solid was placed in a vacuum desiccator overnight to give **16** (hydrochloride salt) (36.27 g, 97%), as a colorless hygroscopic solid, mp 197−199 °C, Anal. (C, H, N). δ_H (400 MHz, DMSO-d_6) 1.02 (9H, s), 3.24 (3H, s), 3.52 (2H, m), 3.61 (1H, d, J 10 Hz), 5.09 (1H, m), 7.25 (1H, t, J 7 Hz), 7.33 (2H, t, J 7 Hz), 7.39 (2H, d, J 7 Hz), 8.05 (3H, bs s), 8.83 (1H, d, J 10 Hz), (LRMS (thermospray) m/z = 265 (MH^+), FTIR $\nu_{max.}$ (KBr disk) 1682, 1559, 1507, 1125, 870, 705 cm^{-1}.

***tert*-Butyl (3*R*)-3-({[(1*S*)-2,2-Dimethyl-1-({[(1*S*)-2-methoxy-1-phenylethyl]amino}carbonyl)propyl]amino}-carbonyl)-6-(3-methyl-4-phenylphenyl)hexanoate (17).** *N*-(Dimethylaminopropyl)-*N*′-ethylcarbodiimide hydrochloride (3.50 g, 18.26 mmol) was added to a stirred mixture of **16** (6.78 g, 17.43 mmol), **13** (6.35 g, 16.6 mmol), 1-hydroxy-1,2,3-benzotriazole hydrate (2.80 g, 20.75 mmol), and diisopropylethylamine (5.9 mL, 34.03 mmol) in anhydrous dichloromethane (82 mL) under nitrogen at 4 °C. After 2 h, the mixture was allowed to warm to room temperature. After 17 h at room temperature, the mixture was poured into ethyl acetate (600 mL), washed sequentially with 5% aqueous citric acid (2 × 250 mL), saturated aqueous sodium bicarbonate (2 × 250 mL), and brine (200 mL), dried ($MgSO_4$), and concentrated under reduced pressure. The residue was redissolved in ether and evaporated to give **17** (10.35 g, 99%), as a colorless foam. Anal. (C, H, N). R_f 0.16 (hexane:ethyl acetate = 4:1). δ_H (400 MHz, $CDCl_3$) 1.02 (9H, s), 1.40 (9H, s and 1H, m, overlapping), 1.55 (2H, m), 1.68 (1H, m), 2.23 (3H, s), 2.32 (1H, m), 2.55 (4H, m), 3.33 (3H, s), 3.62 (2H, d, J = 5 Hz), 4.28 (1H, d, J = 9 Hz), 5.12 (1H, dt, J = 8 and 5 Hz), 6.35 (1H, br d), 6.44 (1H, br d), 6.96 (1H, d, J = 8 Hz), 7.00 (1H, s), 7.10 (1H, d, J = 8 Hz), 7.26 (8H, complex), 7.39 (2H, m). LRMS (thermospray) m/z = 630 (MH^+). FTIR $\nu_{max.}$ (KBr disk) 3320, 2930, 1729, 1643, 1543, 1370, 1157, and 700 cm^{-1}

(3*R*)-3-({[(1*S*)-2,2-Dimethyl-1-({[(1*S*)-2-methoxy-1-phenylethyl]amino}carbonyl)-propyl]amino}carbonyl)-6-(3-methyl-4-phenylphenyl)hexanoic Acid (7). A solution of **17** (535 mg, 0.85 mmol) in anhydrous dichloromethane (5 mL) was treated with trifluoroacetic acid (5 mL) at room temperature for 2 h. The solvents were removed under reduced pressures, and the residue was dissolved in toluene and concentrated under reduced pressure (twice). The residue was recrystallized from ethyl acetate to give a colorless solid (387 mg, 80%). mp 178−180 °C (from ethyl acetate). Anal. (C, H, N). R_f 0.47 (hexane/ether/acetic acid = 50:50:1). δ_H (400 MHz, CD_3OD)(exchangeable hydrogens only partially exchanged) 1.03 (9H, s), 1.51 (4H, m), 2.15 (3H, s), 2.36 (1H, dd, J = 5 and 17 Hz), 2.46 (2H, m), 2.60 (1H, dd, J = 10 and 17 Hz), 2.82 (1H, m), 3.32 (3H, s), 3.57 (2H, d, J = 7 Hz), 4.42 (1H, d, J = 10 Hz), 5.10 (1H, q, J = 7 Hz), 6.87 (1H, d, J = 8 Hz), 6.98 (2H, s and d, J = 8 Hz, overlapping), 7.22 (8H, complex), 7.39 (2H, t, J = 7 Hz), 7.74 (1H, br d), 8.48 (1H, br d). LRMS (thermospray) m/z = 573 (MH^+). FTIR $\nu_{max.}$ (KBr disk) 3300, 2960, 2930, 1711, 1639, 1543, 700 cm^{-1}.

(2*R*)-*N*1-[(1*S*)-2,2-Dimethyl-1-({[(1*S*)-2-methoxy-1-phenylethyl]amino}carbonyl)propyl]-2-{3-(3-methyl-4-phenylphenyl)propyl}-(*N*4-hydroxy)butanediamide (6). (a) *O*-Allylhydroxylamine hydrochloride (81 mg, 0.73 mmol) was added to a stirred solution of (**7**) (347 mg, 0.61 mmol) and diisopropylethylamine (375 μL, 2.19 mmol) in anhydrous dichloromethane (5 mL) under nitrogen at 0 °C. PyAOP (379 mg, 0.73 mmol) was added in one portion, and the mixture was stirred at 0 °C for 2 h and then allowed to warm to room temperature. After an additional 1 h, the mixture was poured into ethyl acetate (50 mL) and washed sequentially with 5% aqueous citric acid (2 × 20 mL) and saturated aqueous sodium bicarbonate (2 × 20 mL). The organic solution was dried (Na_2SO_4) and concentrated under reduced pressure. Purification of the crude product by flash chromatography (eluting with hexane:ethyl acetate = 2:1) followed by trituration with ether and ethyl acetate gave (2*R*)-*N*1-[(1*S*)-2,2-dimethyl-1-({[(1*S*)-2-methoxy-1-phenylethyl]amino}carbonyl)propyl]-2-{3-[(3-methyl-4-phenylphenyl)propyl}-(*N*4-3-propenyloxy)butanediamide (306 mg, 80%) as a white solid, mp 117−120 °C, R_f 0.28 (hexane:ethyl acetate = 1:2), δ_H (400 MHz, $CDCl_3$) 1.02 (9H, s), 1.40−1.70 (4H, complex), 2.20 (3H, s, and 1H, m overlapping), 2.34−2.60 (3H, complex), 2.76 (1H, m), 3.36 (3H, s), 3.63 (2H, d, J = 5 Hz), 4.28 (1H, d, J = 9.5 Hz), 4.34 (2H, d, J = 6 Hz), 5.12 (1H, dt, J = 7.5 and 5 Hz), 5.30 (2H, m), 5.90 (1H, m), 6.44 (1H, d, J = 7.5 Hz and 1H, br s overlapping), 6.94 (1H, m), 6.98 (1H, s), 7.08 (1H, d, J = 7 HZ), 7.18−7.38 (8H, complex), 7.40 (2H, m), 8.50 (1H, br s), LRMS (thermospray) m/z = 628 (MH^+).

(b) A stirred mixture of (2*R*)-*N*1-[(1*S*)-2,2-dimethyl-1-({[(1*S*)-2-methoxy-1-phenylethyl]amino}carbonyl)propyl]-2-{3-[(3-methyl-4-phenylphenyl)propyl}-(*N*4-3-propenyloxy)butanediamide (300 mg, 0.48 mmol) and ammonium formate (300 mg, 4.76 mmol) was dissolved in hot ethanol/water (4:1, 6 mL) to give a colorless solution. A solution of palladium acetate (4 mg, 0.018 mmol) and triphenylphosphine (9.6 mg, 0.037 mmol) in ethanol/water (4:1, 2 mL) was added, and the mixture was heated under reflux for 60 min. After being cooled, the brown solution was diluted with ethyl acetate (100 mL), washed with saturated aqueous sodium chloride (2 × 50 mL), dried ($MgSO_4$), and concentrated under reduced pressure. The residue was purified by column chromatography (C_{18} silanized silica gel (40−63 μm), eluting with methanol:water = 4:1) and then triturated with diisopropyl ether to give **6** (226 mg, 80%) as a white solid, mp 92−96 °C, R_f 0.57 (dichloromethane:methanol:concentrated aq ammonia = 90:10:1); Anal. (C, H, N); δ_H (400 MHz, CH_3OD) 1.02 (9H, s), 1.40−1.68 (4H, m), 2.17 (3H, s), 2.20 (1H, m), 2.36 (1H, m), 2.48 (2H, m), 2.86 (1H, m), 3.30 (3H, s), 3.58 (2H, d, J = 6.5 Hz), 4.40 (1H, s), 5.10 (1H, t, J = 6.5 Hz), 6.88 (1H, m), 6.98 (2H, m), 7.10−7.36 (8H, complex), 7.39 (2H, m); LRMS (thermospray) m/z = 588 (MH^+).

Biology. The assays for MMPs 2, 3, 9, and 14 are based upon the original protocol described by Knight et al.,[57] with the slight modifications given below.

Inhibition of MMP-1. (i) Enzyme Preparation. Catalytic domain MMP-1 was prepared at Pfizer Central Research. A stock solution of MMP-1 (1μM) was activated by the addition of aminophenylmercuric acetate (APMA), at a final concentration of 1 mM, for 20 min at 37 °C. MMP-1 was then diluted in Tris-HCl assay buffer (50 mM Tris, 200 mM NaCl, 5 mM $CaCl_2$, 20 μM $ZnSO_4$, 0.05% Brij 35) pH 7.5 to a concentration of 10 nM. The final concentration of enzyme used in the assay was 1 nM.

(ii) Substrate. The fluorogenic substrate used in this assay was Dnp-Pro-β-cyclohexyl-Ala-Gly-Cys(Me)-His-Ala-Lys(N-Me-Ala)-NH_2.[58] The final substrate concentration used in the assay was 10 μM.

(iii) Determination of Enzyme Inhibition. Test compounds were dissolved in dimethyl sulfoxide and diluted with assay buffer so that no more than 1% dimethyl sulfoxide was present. Test compound and enzyme were added to each well of a 96-well plate and allowed to equilibrate for 15 min at 37 °C in an orbital shaker prior to the addition of substrate. Plates were then incubated for 1 h at 37 °C prior to determination of fluorescence (substrate cleavage) using a fluorimeter (Fluostar; BMG LabTechnologies, Aylesbury, UK) at an excitation wavelength of 355 nm and emission wavelength of 440 nm. The potency of inhibitors was measured from the amount of substrate cleavage obtained using a range of test compound concentrations, and, from the resulting dose−response curve, an IC_{50} value (the concentration of inhibitor required to inhibit 50% of the enzyme activity) was calculated.

Inhibition of MMP-2, MMP-3, and MMP-9. (i) Enzyme Preparation. Catalytic domain MMP-2, MMP-3, and MMP-9 were prepared at Pfizer Central Research. A stock solution of MMP-2, MMP-3, or MMP-9 (1μM) was activated by the addition of aminophenylmercuric acetate (APMA). For MMP-2 and MMP-9, a final concentration of 1 mM APMA was added, followed by incubation for 1 h at 37 °C. MMP-3 was activated by the addition of 2 mM APMA, followed by incubation for 3 h at 37 °C. The enzymes were then diluted in Tris-HCl assay buffer (100 mM Tris, 100 mM NaCl, 10 mM $CaCl_2$ and 0.16% Brij 35, pH 7.5), to a concentration of 10 nM. The final concentration of enzyme used in the assays was 1 nM.

(ii) Substrate.The fluorogenic substrate used in this screen was Mca-Arg-Pro-Lys-Pro-Tyr-Ala-Nva-Trp-Met-Lys(Dnp)-NH_2[59] (Bachem Ltd, Essex, UK). This substrate was selected because it has a balanced hydrolysis rate against MMPs 2, 3, and 9 (k_{cat}/k_m of 54000, 59400, and 55300 s^{-1} M^{-1}, respectively). The final substrate concentration used in the assay was 5 μM.

(iii) Determination of Enzyme Inhibition. Test compounds were dissolved in dimethyl sulfoxide and diluted with test buffer solution (as above) so that no more than 1% dimethyl sulfoxide was present. Test compound and enzyme were added to each well of a 96-well plate and allowed to equilibrate for 15 min at 37 °C in an orbital shaker prior to the addition of substrate. Plates were then incubated for 1 h at 37 °C prior to determination of fluorescence using a fluorimeter (Fluostar; BMG LabTechnologies, Aylesbury, UK) at an excitation wavelength of 328 nm and emission wavelength of 393 nm. The potency of inhibitors was measured from the amount of substrate cleavage obtained using a range of test compound concentrations, and, from the resulting dose−response curve, an IC_{50} value (the concentration of inhibitor required to inhibit 50% of the enzyme activity) was calculated.

Inhibition of MMP-13. (i) Enzyme Preparation. Human recombinant MMP-13 was prepared by PanVera Corporation (Madison, WI) and characterized at Pfizer (Groton, CT). A 1.9 mg/mL stock was activated with 2 mM APMA for 2 h at 37 °C. MMP-13 was then diluted in assay buffer (50 mM Tris, 200 mM NaCl, 5 mM $CaCl_2$, 20 μM $ZnCl_2$, and 0.02% Brij 35) at pH 7.5 to a concentration of 5.3 nM. The final concentration of enzyme used in the assay was 1.3 nM.

(ii) Substrate. The fluorogenic substrate used in this screen was Dnp-Pro-Cha-Gly-Cys(Me)-His-Ala-Lys(NMA)-NH_2. The final substrate concentration used in the assay was 10 μM.

(iii) Determination of Enzyme Inhibition. Test compounds were dissolved in dimethyl sulfoxide and diluted with assay buffer so that no more than 1% dimethyl sulfoxide was present. Test compound and enzyme were added to each well of a 96-well plate. The addition of substrate to each well initiated the reaction. Fluorescence intensity was determined on a 96-well plate fluorometer (Cytofluor II; PerSeptive Biosystems, Inc, Framingham, MA) at an excitation wavelength of 360 nm and emission wavelength of 460 nm. The potency of inhibitors was measured from the amount of substrate cleavage obtained using a range of test compound concentrations, and, from the resulting dose−response curve, an IC_{50} value (the concentration of inhibitor required to inhibit 50% of the enzyme activity) was calculated.

Inhibition of MMP-14. (i) Enzyme Preparation. Catalytic domain MMP-14 was purchased from Prof. Tschesche, Department of Biochemistry, Faculty of Chemistry, University of Bielefeld, Germany. A 10 μM enzyme stock solution was activated for 20 min at 25 °C following the addition of 5 μg/mL of trypsin (Sigma, Dorset, UK). The trypsin activity was then neutralized by the addition of 50 μg/mL of soyabean trypsin inhibitor (Sigma, Dorset, UK), prior to dilution of this enzyme stock solution in Tris-HCl assay buffer (100 mM Tris, 100 mM NaCl, 10 mM $CaCl_2$, and 0.16% Brij 35, pH 7.5) to a concentration of 10 nM. The final concentration of enzyme used in the assay was 1 nM.

(ii) Substrate. The fluorogenic substrate used in this screen was Mca-Pro-Leu-Gly-Leu-Dpa-Ala-Arg-NH_2[60] (Bachem Ltd, Essex, UK). The final substrate concentration used in the assay was 10 μM.

Determination of the Potency of 7 against MMP-3 Using [^{3}H]-Fibronectin. A stock solution of compound **7** in DMSO (10 mM) was diluted in PBS to give a range of assay concentrations, 0.001−30 μM. Plates (96-well) (Costar 3095) were coated with 50 μL/well of a fibronectin solution containing 20 μg/mL unlabeled fibronectin (Collaborative Biomedical Products 40008A) and 5 μCi/mL of [^{3}H]-fibronectin (Amersham, custom preparation; 2.8 mCi/mg) diluted in phosphate buffered saline (PBS). The plates were then sealed, incubated overnight at 37 °C, and subsequently washed three times with PBS to remove any unbound fibronectin. Activated MMP-3 (15 nM in PBS) was prepared as described above and added to a fibronectin-coated plate and incubated with PBS or increasing concentrations of compound **7** (eight wells/inhibitor concentration) at 37 °C overnight. All assays were carried out in a final volume of 100 μL/well. Fifty microliters was withdrawn from each well and added to 4 mL of Starscint (Packard) in a scintillation vial, shaken, and counted using a Wallac 1400 series scintillation counter. From the resulting concentration−% inhibition curve, an IC_{50} value was calculated using FitCurve (Microsoft Excel Tessella Stats add-in).

Determination of the Potency of 7 against MMP-2 and -9 Using [^{3}H]-Gelatin. A stock solution of compound **7** in DMSO (10 mM) was diluted to 1 mM in 3% (w/v) hydroxypropyl-β-cyclodextrin and then in PBS to give a range of assay concentrations, 0.001−30 μM. A [^{3}H]-gelatin solution was prepared by denaturing a [^{3}H]-collagen solution containing 1.5 μg/mL collagen type III and 0.5 μCi/mL of [^{3}H]-collagen by heating at 60 °C for 2 h. Plates (96-well) (Costar 3590) were then coated with 50 μL/well of this solution, and the supernatant was evaporated for 96 h at 37 °C in a sealed container containing silica gel. Plates were then initially washed three times (10 min per wash) with PBS, one wash by incubation with PBS for 2 h at 37 °C, and finally a further three washes (10 min each) with PBS to remove any unbound gelatin. Activated MMP-2 or -9 (1 nM in PBS) was prepared as described above and added to a gelatin-coated plate and incubated with PBS or increasing concentrations of compound **7** (eight wells/inhibitor concentration) at 37 °C overnight. All assays were carried out in a final volume of 200 μL/well. The whole sample was withdrawn from each well and added to 4 mL of Starscint (Packard) in a scintillation vial, shaken, and counted using a Wallac 1400 series scintillation counter. From the resulting concentration−% inhibition curve, an IC_{50} value was calculated using FitCurve (Microsoft Excel Tessella Stats add-in).

Effects of Compound 7 on Human Keratinocyte Cell Migration in Vitro. A stock solution of compound **7** in DMSO (10 mM) was diluted with Keratinocyte Growth Medium-2 (KGM-2) to give a range of assay concentrations 0.01−100 μM. One piece of sterile Flexiperm (Heraeus Instruments) was placed into each well of a collagen coated 12-well tissue culture plate (Becton Dickinson), with the smooth side adhering to the well base. Normal adult human epidermal keratinocytes (Clonetics, CC-2501 − batch NHEK 2199) were then seeded into the Flexiperm at a density of 5×10^4 cells/well in 200 μL of KGM-2. When cells reached 90% confluence (48 h after seeding), the Flexiperm was removed from the plate and 1 mL of growth medium, containing compound **7** at 0.01−100 μM (or vehicle), was added to quadruplicate wells. The limit of solubility of **7** in this assay system was 100 μM. Experiments were performed in the presence of 5-fluoro-5′-deoxyuridine (40 μM), to prevent cell proliferation. The initial diameter of each cell circle was measured by phase contrast microscopy using an eyepiece graticule. Plates were then incubated for 96 h at 37 °C in 5% CO_2 in air to permit the keratinocytes to migrate, and the final diameter of the cell circle was measured. Inhibition of migration was calculated by determining the distance migrated (final cell circle diameter less initial cell circle diameter) and comparison to the vehicle control. Experiments were performed in triplicate. Data in Table 2 is expressed as the mean percentage inhibition of migration (± SEM) of triplicate experiments, relative to vehicle controls.

Rabbit Adriamycin-Induced Wound Healing Model. Animal husbandry and scientific procedures were conducted in a manner consistent with U.K. legislation and approved by the local ethical review process prior to commencement of the study. Healthy male New Zealand White rabbits (2−2.5 kg) were weighed and acclimated in individual cages for at least 7 days prior to the study. The rabbits were sedated with medetomidine (250 μg/kg im) and the hair clipped from the dorsal midline. Adriamycin (Farmitalia Carlo Erba Ltd)(500 μL of 1 mg/mL dissolved in physiological saline) was administered id at six sites. Once adriamycin had been administered, burenorphine (0.02 mg/kg sc) was given for analgesia. Subsequently, the rabbits' sedation was reversed using an im injection of 1.25 mg/kg of atipamezole. Full recovery was routinely seen within 5 min.

Seven days after adriamycin injection the rabbits were reanaesthetised as above, coloplasts (Cohesive stoma seals, Salts Healthcare) were glued (Vetbond, 3M) in place around each wound, and compound **7** was then dosed topically to the wound, formulated as a suspension in an aqueous hydrogel (Intrasite, Smith and Nephew) (0.5 mL, 30 or 10 mg/mL). The wounds were then occlusively dressed using Opsite (Johnson & Johnson), and the rabbits were wrapped with Vetwrap (3M) to prevent interference with the wounds and dressings.

For determination of inhibition of MMP-3, three rabbits were dosed on day 7 such that eight wounds received 15 mg per wound, seven wounds received 5 mg per wound, and three wounds received only Intrasite hydrogel vehicle. Each animal had one vehicle treated wound and a mixture of 15 mg and 30 mg doses. These wounds were dressed occlusively and left for 3 days, after which the dose was removed and the wounds were redosed with a maintenance dose of half the original amount. The wounds were redressed and left for a further 3 days after which the animals were euthanized and the wounds harvested.

Each wound was dissected for subsequent pharmacodynamic and pharmacokinetic analysis by first bisection vertically through the wound from top to bottom, and for the pharmacokinetic analysis, the half of the wound was further bisected horizontally to divide the sample into top and bottom portions. The wound was not further bisected for the pharmacodynamic analysis.

Pharmacokinetics in Rabbit Chronic Dermal Wounds. The dissected wounds were weighed and homogenized in 500 μL of buffer (100 mM Tris, 15 mM $CaCl_2$, pH 7.5), and 0.1 mL aliquots of rabbit wound homogenate were extracted with ethyl acetate (5 mL). The supernatant was removed and evaporated under a nitrogen stream. Each sample was redissolved in HPLC mobile phase (100 μL) of which 80 μL was injected onto the HPLC column (Hypersil BDS C18 (5 μm, 25 cm × 4.6 mm id), eluting with 60% MeCN/40% water (0.1% trifluoroacetic acid), 1.5 mL/min, UV detection at 205 nm. The assay has a calibration range of 0.5−200 μg/mL using a quadratic fit, and all standards were prepared by addition of known concentrations of compound **7** to 0.1 mL aliquots of rat plasma. Samples outside the calibration range were diluted for analysis.

Measurement of Inhibition of MMP-3 in Rabbit Chronic Dermal Wounds. Harvested wounds were stored at −70 °C prior to analysis. The frozen wounds were bisected, trimmed of surrounding normal skin, and mounted wound face uppermost in embedding medium (Tissue-Tek 4583). The tissue was cut into rectangular blocks measuring approximately 10 × 5 × 20 mm. Full-width 15 μm Cryostat (Leica CM1100) sections were then cut for addition to the assay plate (96-well clear-bottomed fluorimeter plates (Costar 3631)). Each well in the assay plate contained assay buffer (pH 7.5 100 mM Tris Base, 100 mM NaCl, 10 mM $CaCl_2$, 0.05% Brij 35, 50 μL total volume) with a proprietary serine and cysteine protease inhibitor cocktail ((Boehringer-Mannheim 1873580, one tablet reconstituted in 25 mL of assay buffer) to eliminate substrate cleavage by non-MMP enzymes. Each wound was assayed in 16 replicates ± compound **2** (a nonselective MMP inhibitor, 100 μM) to determine MMP activity in each section. This was necessary, as there was an activity present within the sections that was not inhibited by the cocktail or compound **2** and so is therefore not MMP-dependent.

Prior to section addition, the plate was exposed to an antistatic charge (Zerostat 3, Aldrich Z-108812) to aid insertion of the wound section into the well. Once all sections were added, the plate was sealed (Costar 6524) and incubated for 15 min at 37 °C. Substrate (Mca-Arg-Pro-Lys-Pro-Val-Glu-Nva-Tyr-Arg-Lys(Dnp)NH_2, (Bachem M-2110) for MMP-3) was then added to all wells, and the plate was resealed and then read kinetically (BMG Fluostar 96-well plate fluorimeter) from the bottom for 4 h with readings taken every 5 min.

Results calculation for MMP-3 assay:

The mean reaction velocity (V) for each of 16 wells was calculated for the first 75 min of the assay to ensure the curves were linear and then averaged (Tessella stats Excel add-in) for each wound ± compound **2**. This yielded $n = 1$ (one wound). MMP activity present in each sample was calculated according to the following formula:

sample MMP activity = sample mean V − (sample + compound **2** mean V)

Data were excluded if Grubbs's test showed the data was significantly discordant at the 1% level. The sample MMP activity was used to calculate % inhibition in the dosed wounds

with respect to vehicle MMP activity. Statistical differences between the data sets was analyzed using a two-sided unpaired *t*-test (Tessella Stats Excel add-in).

Acknowledgment. The authors wish to thank T. J. Evans and C. A. Loosley for compound synthesis. E. Fairman, K. Holland, S. D. Lewis, J. Owen (Sandwich laboratories), and Dr. P. McCarthy and L. Reeves (Groton laboratories) measured enzyme inhibition potencies. We also thank M. G. Collis for advice, and B. I. Williams-Jones, H.C.W. Williams-Jones, E. Newstead, R. Webster, J. Phipps (née Taberner), and D. McCleverty for additional in vitro experiments and in vivo pharmacokinetic and pharmacodynamic studies. We are grateful to N. M. Thomson and A. M. Derrick for developing the selective Suzuki reaction to make compound **7**, and the staff of the Structure and Separation Sciences department for measuring spectroscopic data. We are particularly indebted to Prof. J. M. Davidson, Department of Pathology, Vanderbilt University, Nashville, TN, for a collaboration to develop the rabbit model of chronic wound healing.

References

(1) Martin, P., Wound healing − aiming for perfect skin regeneration. *Science* **1997**, *276*, 75−81.
(2) Falanga, V. Chronic wounds − pathophysiologic and experimental considerations. *J. Invest. Dermatol.* **1993**, *134*, 721−725.
(3) Ruckley, C. V.; Socioeconomic impact of chronic venous insufficiency and leg ulcers. *Angiology* **1997**, *48*, 67−69.
(4) Mayberry, J. C.; Moneta, G. L.; Taylor, L. M.; Porter, J. M. 15-year results of ambulatory compression therapy for chronic venous ulcers. *Surgery* **1991**, *109*, 575−581.
(5) Tarnuzzer, R. W.; Macauley, S. P.; Mast, B. A.; Gibson, J. S.; Stacey, M. C.; Trengrove, N.; Moldawer, L. L.; Burslem, F.; Schultz, G. S. Epidermal growth factor in wound healing: a model for the molecular pathogenesis of chronic wounds. *Growth factors and wound healing*; Springer-Verlag: New York, 1997; Chapter 12, pp 206−228.
(6) Saarialho-Kere, U. K. Patterns of matrix metalloproteinase and TIMP expression in chronic ulcers. *Arch. Dermatol. Res.* **1998**, *290*, Suppl: S47−54.
(7) Tarnuzzer, R. W.; Schultz, G. S. Biochemical analysis of acute and chronic wound environments. *Wound Rep. Regul.* **1996**, *4*, 321−325.
(8) Bucalo, B.; Englstein, W. H.; Falanga, V. Inhibition of cell proliferation by chronic wound fluid. *Wound Rep. Regul.* **1993**, *1*, 181−186.
(9) Herrick, S. E.; Ireland, G. W.; Simon, D.; McCollum, C. N.; Ferguson, M. W. J. Venous ulcer fibroblasts compared with normal fibroblasts show differences in collagen but not fibronectin production under both normal and hypoxic conditions. *J. Invest. Dermatol.* **1996**, *106*, 187−193.
(10) Grinnell, F.; Ho, C. H.; Wysocki, A. Degradation of fibronectin and vitronectin in chronic wound fluid: analysis by cell blotting, immunoblotting, and cell adhesion assays. *J. Invest. Dermatol.* **1992**, *98*, 410−416.
(11) Alper, J. C.; Tibbetts, L. L.; Sarazen, A. A. J. The in vitro response of fibroblasts to the fluid that accumulates under a vapour-permeable membrane. *J. Invest. Dermatol.* **1985**, *84*, 513−515.
(12) Wilhelm, S. M.; Collier, I. E.; Kronberger, A.; Elsen, A. Z.; Barry, L.; Gregory, A.; Bauer, E. A.; Goldberg, G. I. Human skin fibroblast stromelysin: structure, glycosylation, substrate specificity, and differential expression in normal and tumorigenic cells. *Proc. Nat. Acad. Sci. U.S.A.* **1987**, *84*, 6725−6729.
(13) Mast, B. A.; Schultz, G. S. Interactions of cytokines, growth factors and proteases in acute and chronic wounds. *Wound Rep. Regul.* **1996**, *4*, 411−420.
(14) Saarialho-Kere, U. K.; Pentland, A. P.; Birkedal-Hansen, H.; Parks, W. C.; Welgus, H. G.; Distinct populations of basal keratinocytes express stromolysis-1 and stromolysis-2 in chronic wounds, *J. Clin. Invest.* **1994**, *94*, 79−87.
(15) Vaalamo, M.; Weckroth, M.; Puolakkainen, P.; Kere, J.; Saarinen, P.; Lauharanta, J.; Saarialho-Kere, U. K.; Patterns of matrix metalloproteinase and TIMP-1 expression in chronic and normally healing human cutaneous wounds. *Br. J. Dermatol.* **1996**, *135*, 52−59.
(16) Weckroth, M.; Vaheri, A.; Lauharanta, J.; Sorsa, T.; Konttinen, Y. T. Matrix metalloproteases, gelatinase and collagenase, in chronic dermal ulcers. *J. Invest. Dermatol.* **1996**, *106*, 1119−1124.
(17) Wysocki, A. B.; Stainocoico, L.; Grinnel, F. Wound fluid from chronic leg ulcers contains elevated levels of metalloproteases MMP-2 and MMP-9. *J. Invest. Dermatol.* **1993**, *101*, 64−68.
(18) Mast, A. E.; Enghild, J. J.; Nagase, H.; Suzuki, K.; Pizzo, S. V.; Salvesen, G. Kinetics and physiological relevance of the inactivation of alpha 1-proteinase inhibitor, alpha 1-antichymotrypsin, and antithrombin III by matrix metalloproteinases-1 (tissue collagenase), -2 (72kDa gelatinase/type IV collagenase), and -3 (stromelysin). *J. Biol. Chem.* **1991**, *266*, 15810−15816.
(19) Rao, C. N.; Ladin, D. A.; Liu, Y. Y.; Chilukuri, K.; Hou, Z. Z.; Woodley, D. T. α1-antitrypsin is degraded and nonfunctional in chronic wounds but intact and functional in acute wounds: the inhibitor protects fibronectin from degradation by chronic wound fluid enzymes. *J. Invest. Dermatol.* **1995**, *105*, 572−578.
(20) Hoffman, R.; Noble, J.; Eagle, M. The use of proteases as prognostic markers for the healing of venous leg ulcers. *J. Wound Care* **1999**, *8*, 273−276.
(21) Pei, D.; Majmundar, G.; Weiss, S. J. Hydrolytic inactivation of a breast carcinoma cell-derived serpin by human stromelysin-3. *J. Biol. Chem.* **1994**, *269*, 25849.
(22) Bullard, K. M.; Lund, L.; Mudgett, J. S.; Mellin, T. N.; Hunt, T. K.; Murphy, B.; Ronan, J.; Werb, Z.; Banda, M. J. Impaired Wound Contraction in Stromelysin-1-Deficient Mice. *Ann. Surgery* **1999**, *230*, 260−5.
(23) For recent reviews, see Wojtowicz-Praga, S.; Clinical potential of matrix metalloprotease inhibitors. *Drugs R&D* **1999**, *1*, 117−129. De, B.; Natchus, M. G.; Cheng, M.; Pikul, S.; Almstead, N. G.; Taiwo, Y. O.; Snider, C. E.; Chen, L.; Barnett, B.; Gu, F.; Dowty, M. The next generation of MMP inhibitors: design and synthesis. *Ann. N. Y. Acad. Sci.* **1999**, *878* (Inhibition of Matrix Metalloproteinases), 40−60. Whittaker, M.; Floyd, C. D.; Brown, P.; Gearing, A. J. H. Design and Therapeutic Applications of Matrix Metalloprotease Inhibitors. *Chem. Rev.* **1999**, *99*, 2735−2776. Johnson, L. L.; Dyer, R.; Hupe, D. J. Matrix metalloproteases *Curr. Opin. Chem. Biol.* **1998**, *2*, 466. Babine, R. E.; Bender, S. L. Molecular Recognition of Protein−Ligand Complexes: Applications to Drug Design. *Chem. Rev.* **1997**, *97*, 1359.
(24) Saarialho-Kere, U. K.; Kovacs, S. O.; Pentland, A. P. Cell−matrix interaction modulate interstitial collagenase expression by human keratinocytes actively involved in wound healing. *J. Clin. Invest.* **1993**, *92*, 2858−66.
(25) Pilcher, B. K.; Dumin, J. A.; Sudbeck, B. D.; Krane, S. M.; Welgus, H. G.; Parks, W. C. The activity of collagenase-1 is required for keratinocyte migration on a type I collagen matrix. *J. Cell Biol.* **1997**, *137*, 1445−57.
(26) Agren, M. S. Gelatinase activity during wound healing. *Brit. J. Dermatology* **1994**, *131*, 634−40.
(27) Salo, T.; Mäkänen, M.; Kylmäniemi, M.; Autio-Harmainen, H.; Larjava, H. Expression of matrix metalloproteinase-2 and -9 during early human wound healing. *Lab. Invest.* **1994**, *70*, 176−82.
(28) Taraboletti, G.; Garofalo, A.; Belotti, D.; Drudis, T.; Borsotti, P.; Scanziani, E.; Brown, P. D.; Giavazzi, R. Inhibition of angiogenesis and murine hemangioma growth by batimastat, a synthetic inhibitor of matrix metalloproteinases. *J. Natl. Cancer Inst.* **1995**, *87*, 293−8.
(29) Cook, H.; Stephens, P.; Davies, K. J.; Harding, K. G.; Thomas, D. W. Defective extracellular matrix reorganization by chronic wound fibroblasts is associated with alterations in TIMP-1, TIMP-2 and MMP-2 activity. *J. Invest. Dermatol.* **2000**, *115*, 225−233.
(30) Wall, S.; Murphy, G.; Matrix metalloproteinase expression in impaired wound healing. *Int. J. Exp. Pathol.* **2000**, *81*, A27.
(31) Takino, T.; Sato, H.; Shinagawa, A.; Seiki, M. Identification of the second membrane-type matrix metalloproteinase (MT-MMP-2) gene from a human placenta cDNA library. MT-MMPs form a unique membrane-type subclass in the MMP family. *J. Biol. Chem.* **1995**, *270*, 23013−20.
(32) Vaalamo, M.; Mattila, L.; Johansson, N.; Kariniemi, A. L.; Karjalainen-Lindsberg, M. L.; Kahari, V. M.; Saarialho-Kere U. Distinct populations of stromal cells express collagenase-3 (MMP-13) and collagenase-1 (MMP-1) in chronic ulcers but not in normally healing wounds. *J. Invest. Dermatol.* **1997**, *109*, 96−101.
(33) Scott, K. A.; Wood, E. J.; Karran, E. H. A Matrix Metalloprotease Inhibitor which prevents Fibroblast-mediated Collagen Lattice Contraction. *FEBS Lett.* **1998**, *441*, 137−140.
(34) Pilcher, B. K.; Wang, M.; Qin, X.-J.; Parks, W. C.; Senior, R. M.; Welgus, H. G. Role of matrix metalloproteinases and their inhibition in cutaneous wound healing and allergic contact hypersensitivity. *Ann. N. Y. Acad. Sci.* **1999**, *878*, 12−24.

(35) Mirastschijski, U.; Impola, U.; Karsdal M. A.; Saarialho-Kere, U.; Agren, M. S. Matrix metalloproteinase inhibitor BB-3103 unlike the serine proteinase inhibitor aprotinin abrogates epidermal healing of human skin wounds ex vivo. *J. Invest. Dermatol.* **2002**, *118*, 55−64.
(36) Agren, M. S. Matrix metalloproteinases (MMPs) are required for re-epithelialization of cutaneous wounds. *Arch. Dermatol. Res.* **1999**, *291*, 583−590.
(37) Agren M. S.; Mirastschijski U.; Karlsmark T.; Saarialho-Kere U. K.; Topical synthetic inhibitor of matrix metalloproteinases delays epidermal regeneration of human wounds. *Exp. Dermatol.* **2001**, *10*, 337−48.
(38) Stocker, W.; Grams, F.; Baumann, U.; Reinmer, P.; Gomis-Ruth, F.; McKay, D.; Bode, W.; The Metzincins − Topological and Sequential Relations between the Astacins, Adamalysins, Serralysins, and Matrixins (Collagenases) Define a Superfamily of Zinc-Peptidases. *Protein Sci.* **1995**, *4*, 823−840.
(39) Kessler, E.; Takahara, T.; Biniamov, L.; Brusel, M.; Greenspan, D. S. Bone Morphogenetic Protein-1: The Type-1 Procollagen C−Proteinase. *Science* **1996**, *271*, 360−362.
(40) Fray, M. J.; Burslem, M. F.; Dickinson, R. P. Selectivity of Inhibition of Matrix Metalloproteases MMP-3 and MMP-2 by Succinyl Hydroxamates and their Carboxylic Acid Analogues is Dependent on P3′ Group Chirality. *Bioorg. Med. Chem. Lett.* **2001**, *11*, 567−570.
(41) Fray, M. J.; Dickinson, R. P. Discovery of Potent and Selective Succinyl Hydroxamate Inhibitors of Matrix Metalloprotease-3 (Stromelysin-1). *Bioorg. Med. Chem. Lett.* **2001**, *11*, 571−574.
(42) Bird, J.; Montana, J. G.; Wills, R. E.; Baxter, A. D.; Owen, D. A. World Patent Appl., 1998, WO 98/39024; *Chem. Abstr. 129*, 225751.
(43) Plattner, J. J.; Marcotte, P. A.; Kleinert, H. D.; Stein, H. H.; Greer, J.; Bolis, G.; Fung, A. K. L.; Bopp, B. A.; Luly, J. R.; Sharn, H. L.; Kempf, D. J.; Rosenberg, S. H.; Dellaria, J. F.; Merits, I.; Perun, T. J. Renin inhibitors. Dipeptide analogues of angiotensinogen utilizing a structurally modified phenylalanine residue to impart proteolytic stability. *J. Med. Chem.* **1988**, *31*, 2277−88.
(44) Evans, D. A.; Wu, L. D.; Wiener, J. J. M.; Johnson, J. S.; Ripin, D. H. B.; Tedrow, J. S. A general method for the synthesis of enantiomerically pure β-substituted, β-amino acids through α-substituted succinic acid derivatives. *J. Org. Chem.* **1999**, *64*, 6411−6417.
(45) Gomberg, M.; Pernert, J. C. Methylbiphenyls. *J. Am. Chem. Soc.* **1926**, *48*, 1372−1384.
(46) Pattenden, G.; Teague, S. J. Transannular cyclization as a strategem in synthesis. Total synthesis of (±)-pentalenene. *Tetrahedron* **1987**, *43*, 5637−5652.
(47) Savino, T. G.; Kanakarajan, K.; Platz, M. S. Unusual temperature-dependent isotope effects in the reactions of phenylcarbene with cyclohexene and cyclohexane. *J. Org. Chem.* **1986**, *51*, 1305−1309.
(48) Smith, A. B., III; Yager, K. M.; Taylor, C. M. Enantioselective synthesis of diverse α-amino phosphonate diesters. *J. Am. Chem. Soc.* **1995**, *117*, 10879−10888.
(49) Pospisek, J.; Blaha, K. Amino acids and peptides. CXXXIX. tert-Leucine and its simple peptides. *Collect. Czech. Chem. Commun.* **1977**, *42*, 1069−1076.
(50) Makela, M.; Larjava, H.; Pirila, E.; Maisi, P.; Salo, T.; Sorsa, T.; Uitto, V. J. Matrix metalloproteinase 2 (gelatinase A) is related to migration of keratinocytes. *Exp. Cell Res.* **1999**, *251*, 67−78.
(51) McCawley, L. J.; O'Brien, P.; Hudson, L. G. Epidermal growth factor (EGF)- and scatter factor/hepatocyte growth factor (SF/HGF)- mediated keratinocyte migration is co-incident with induction of matrix metalloproteinase (MMP)-9. *J. Cell. Physiol.* **1998**, *176*, 255−265.
(52) Esser, C. K.; Bugianesi, R. L.; Caldwell, C. G.; Chapman, K. T.; Durette, P. L.; Giotra, N. N.; Kopka, I. E.; Lanza, T. J.; Levorse, D. A.; MacCoss, M.; Owens, K. A.; Ponpipom, M. M.; Simeone, J. P.; Harrison, R. K.; Niedzwiecki, L.; Becker, J. W.; Marcy, A. I.; Axel, M. G.; Christen, A. J.; McDonnell, J.; Moore, V. L.; Olszewski, J. M.; Saphos, C.; Visco, D. M.; Shen, F.; Colletti, A.; Krieter, P. A.; Hagmann, W. K. Inhibition of stromelysin-1 (MMP-3) by P1′-biphenylethyl carboxyalkyl dipeptides. *J. Med. Chem.* **1997**, *40*, 1026.
(53) Chapman, K. T.; Durette, P. L.; Caldwell, C. G.; Sperow, K. M.; Niedzwiecki, L.; Harrison, R. K.; Saphos, C.; Christen, A. J.; Olszewski, J. M.; Moore, V. L.; MacCoss, M.; Hagmann, W. K. Orally active inhibitors of stromelysin-1 (MMP-3). *Bioorg. Med. Chem. Lett.* **1996**, *6*, 803.
(54) Bender, S. Presentation at The Second Winter Conference on Medicinal and Bioorganic Chemistry, Steamboat Springs, CO, Jan 26−31, 1997.
(55) Davidson, Prof. J. M. unpublished work. A delayed healing wound model in the rat has also been described; see Chen, C.; Schultz, G. S.; Bloch, M.; Edwards, P. D.; Tebes, S.; Mast, B. A. Molecular and mechanistic validation of delayed healing rat wounds as a model for human chronic wounds. *Wound Rep. Regul.* **1999**, *7*, 486-494, and a model of wound healing in diabetic pigs, see M. C. Niciporciukas, World Patent WO 98/57169, 1998.
(56) Beekman, B.; van El, B.; Drijfhout, J. W.; Ronday, H. K.; TeKoppele, J. M. Highly increased levels of active stromelysin in rheumatoid synovial fluid determined by a selective fluorogenic assay. **1997**, *FEBS Lett. 418*, 305−309.
(57) Knight, C. G.; Wilenbrock, F.; Murphy, G.; A novel coumarin-labeled peptide for sensitive continuous assays of the matrix metalloproteinases. *FEBS Lett.* **1992**, *296*, 263−266.
(58) Bickett, D. M.; Green, M. D.; Berman, J.; Dezube, M. A high throughput fluorogenic substrate for interstitial collagenase (MMP-1) and gelatinase (MMP-9). *Anal. Biochem.* **1993**, *212*, 58−64.
(59) Nagase, H.; Fields, C. G.; Fields, G. B. Design and characterization of a fluorogenic substrate selectively hydrolyzed by stromelysin-1 (matrix metalloproteinase −3). *J. Biol. Chem.* **1994**, *269*, 20952−20957.
(60) Will, H.; Atkinson, S. J.; Butler, G. S.; Smith, B.; Murphy, G. The soluble catalytic domain of membrane type-1 matrix metalloproteinase cleaves the propeptide of progelatinase A and initiates auto proteolytic activation. Regulation by TIMP 2 and TIMP 3. *J. Biol. Chem.* **1996**, *271*, 17119−17123.

JM0308038